Research paper

Tissue-specific effects of targeted mutation of *Mir29b1* in rats

Hong Xue [a,b,*,1], Guangyuan Zhang [b,1], Aron M. Geurts [b], Kristie Usa [b], David M. Jensen [b], Yong Liu [b], Michael E. Widlansky [c], Mingyu Liang [b,*]

[a] Department of Physiology and Pathophysiology, Fudan University Shanghai Medical College, Shanghai, PR China
[b] Center of Systems Molecular Medicine, Department of Physiology, Medical College of Wisconsin, Milwaukee, WI, USA
[c] Departments of Medicine and Pharmacology, Division of Cardiovascular Medicine, Medical College of Wisconsin, Milwaukee, WI, USA

ARTICLE INFO

ABSTRACT

Background: miR-29 is a master regulator of extracellular matrix genes, but conflicting data on its anti-fibrotic effect have been reported. miR-29 improves nitric oxide (NO) production in arterioles by targeting Lypla1. *Mir29b1* targeted mutation exacerbates hypertension in a model derived from the Dahl salt-sensitive rat. We examined the effect of *Mir29b1* mutation on tissue fibrosis and NO levels with a focus on kidney regions.
Methods: *Mir29b1* targeted mutant rats on the genetic background of SS-Chr13[BN] rats were studied. Masson trichrome staining, molecular and biochemical assays, metabolic cage studies, and bioinformatic analysis of human genomic data were performed.
Findings: The abundance of miR-29b and the co-transcribed miR-29a was substantially lower in mutant rats. Tissue fibrosis was significantly increased in the renal outer medulla, but not in the renal cortex, heart or liver in mutant rats on a 0.4% NaCl diet. Lypla1 protein abundance was significantly higher and NO levels lower in the renal outer medulla, but not in the renal cortex. After 14 days of a 4% NaCl diet, 24 h urine volume and urinary sodium excretion was significantly lower in mutant rats, and tissue fibrosis became higher in the heart. NO levels were lower in the renal outer medulla and heart, but not in the renal cortex. Human miR-29 genes are located in proximity with blood pressure-associated single nucleotide polymorphisms.
Interpretation: The renal outer medulla might be particularly susceptible to the injurious effects of a miR-29 insufficiency, which might contribute to the development of hypertension in *Mir29b1* mutant rats.

1. Introduction

MicroRNAs are endogenous, conserved, small non-coding RNAs that block translation or induce degradation of target mRNA. The miR-29 family is highly conserved among mammalian species [1]. The family comprises of three variants, miR-29a, miR-29b and miR-29c. The gene encoding the co-transcribed precursors of miR-29b-1 and miR-29a is located on chromosome 7q32.3 in the human genome, while the gene encoding the precursors of miR-29b-2 and miR-29c is located on chromosome 1q32.2. In rat, miR-29b-1 and miR-29a are clustered on chr. 4 and miR-29b-2 and miR-29c on chr. 13.

Strong antifibrotic effects of miR-29s have been demonstrated in multiple organs [2], including heart [3, 4], liver [5, 6] and kidney [7, 8]. Antagonism of miR-29 in vivo resulted in increased collagen in the cardiac tissue, whereas introduction of miR-29 mimics after heart damage reduced the collagen content [3]. Upregulation of miRNA-29a either by enforced overexpression or by the use of carvedilol, a beta-adrenoreceptor antagonist, was shown to reduce myocardial fibrosis mediated by experimental myocardial infarction in rat [9]. In the liver, overexpression of miR29a through systemic adenoviral delivery ameliorated hepatic fibrosis induced by carbon tetrachloride [10].

In the kidney, our previous study demonstrated that miR-29 regulated a large number of collagens and other genes related to the extracellular matrix in Dahl salt-sensitive (SS) rats [11], the most widely used polygenetic model of human salt-sensitive forms of hypertension and renal injury [12, 13]. miR-29b was elevated in the renal medulla of the consomic SS-Chr13[BN] rats in response to a high-salt diet, but not in SS rats. The SS-Chr13[BN] rat is a consomic strain derived from the SS rat, in which chromosome 13 of the SS genome has been replaced by chromosome 13 from the Brown Norway (BN) rat, and exhibits substantially attenuated hypertension and renal injury [14]. We recently developed *Mir29b1* mutant rats ($Mir29b$-$1/a^{-/-}$) on the background of the SS-Chr13[BN] rat by deleting four base pairs in the genomic segment of the *Mir29b-1/a* gene that encodes nucleotides 6–9 in the sequence of mature miR-29b-3p [15]. This was the first targeted

Research in context

MicroRNAs are endogenous non-coding RNAs that regulate, mainly suppress, the expression of target genes. miR-29 targets approximately 20 genes related to extracellular matrix, which is one of the most dramatic examples of a miRNA coordinately targeting a large number of genes that belong to a single pathway. Exciting progress is being made in the development of miR-29-based therapeutic approaches. For instance, miR-29b mimic treatment blunts bleomycin-induced pulmonary fibrosis. However, conflicting data on whether miR-29 is anti-fibrotic have been reported.

We recently developed a miR-29b1 targeted mutant rat strain, which was the first reported microRNA mutant rat strain to our knowledge. This unique model enabled us to examine the role of miR-29 in various tissues under normal and disease conditions. We found the renal outer medulla was particularly sensitive to the injurious effects of the miR-29 insufficiency. Decreased nitric oxide via the miR-29/Lypla1 pathway provides a possible explanation for the tissue-specific effect of miR-29 and new insights into how miR-29 might contribute to the regulation of blood pressure response to dietary salt intake. Human miR-29 genes are among a small number of microRNA genes that are located in proximity with blood pressure-associated single nucleotide polymorphisms, suggesting potential relevance of miR-29 to the genetic determinants of human blood pressure. The study significantly advances the understanding of the tissue- and disease context-specificity of the effect of miR-29. It also highlights the importance of considering such specificity for therapeutic purposes.

microRNA mutant rat ever reported to our knowledge. $Mir29b\text{-}1/a^{-/-}$ rats on a high-salt diet developed significantly exacerbated hypertension compared to $Mir29b\text{-}1/a^{+/+}$ littermates. Using arterioles from $Mir29b\text{-}1/a^{-/-}$ rats as well as humans, we showed miR-29 increased NO production by targeting lysophospholipase I (Lypla1). Lypla1 would otherwise de-palmitoylate endothelial nitric oxide synthase (eNOS) and inhibit eNOS activities [15].

The kidney, particularly the renal outer medulla, plays a key role in the development of salt-sensitive hypertension [16–19]. Renal injury precedes overt hypertension in the SS rats [20, 21]. NO has protective effects against tissue injury and fibrosis [22–24]. Renal NO inhibits tubular reabsorption of fluid and sodium, which may contribute to the anti-hypertensive effect of NO [25–27]. To further understand the role of miR-29 in the development of tissue fibrosis and salt-sensitive hypertension, we examined changes in tissue fibrosis and NO levels in $Mir29b\text{-}1/a^{-/-}$ rats with a focus on kidney regions in the present study. Bioinformatic analysis was performed to examine the potential relevance of miR-29 to genetic determinants of blood pressure variations in humans.

2. Methods

2.1. Mir29b-1 mutant rats

A custom-made Transcriptional Activator-Like Effector Nucleases (TALENs) method was used to target the *Mir29b-1* gene on the genetic background of SS-Chr13^BN rats [28]. The protocol has been described in detail in our previous study [15]. Briefly, four nucleotides overlapping the seed region, which is critical for the function of miR-29b, were deleted in *Mir29b-1/a* mutant rat. Heterozygous breeder pairs were setup, giving rise to litters containing wild-type (*Mir29b-1/a^{+/+}*), heterozygous (*Mir29b-1/a^{+/−}*), and homozygous (*Mir29b-1/a^{−/−}*) mutant rats. Rats were maintained on the AIN-76A diet containing 0.4% NaCl

(Dyets). Male rats were used for experiments at 8 weeks of age. The animal study was approved by the Institutional Animal Care and Use Committee at the Medical College of Wisconsin.

2.2. Tissue and urine collection

On the day of tissue harvest, rats were anesthetized with intramuscular injection of a mixture of ketamine (75 mg/kg), xylazine (10 mg/kg), and acepromazine (2.5 mg/kg). Liver, heart and kidneys were removed quickly. Half of right kidney was fixed in neutral formalin. Renal cortex, outer medulla and inner medulla were selectively dissected using the remaining kidney tissue, snap frozen in liquid nitrogen, and stored at −80 °C. For urine collection, animals were moved into metabolic cages for 24 h. Urine volume was recorded and urine samples were stored at −80 °C until analysis.

2.3. Renal morphological analyses

Analysis of tissue fibrosis was performed with 3 μm paraffin-embedded sections stained by Masson trichrome as we described previously [29]. The positive-stained area of collagens was quantitatively measured using a computer-aided image system on digitized images that were transformed from analog images taken by a camera.

2.4. RNA isolation

Total RNA was extracted from tissues with Trizol reagent (Invitrogen, USA). RNA concentration was measured using a NanoDrop spectrophotometer (NanoDrop Technologies, USA).

2.5. Measurement of miR-29s using TaqMan real-time PCR

Total RNA samples were used to measure abundance of miR-29a, b and c using modified real-time PCR with TaqMan (Applied Biosystems) chemistry, as described previously [15, 30]. 5S rRNA was used as an internal normalizer.

2.6. Western blot for Lypla1

Western blot was performed as we described previously [14, 31]. Primary antibody for LYPLA1 was from Sigma Aldrich (SAB2101408, rabbit polyclonal), and used at 1:500 dilution. The density of a specific band was normalized by Coomassie blue staining of the entire lane [15, 31] [32].

2.7. Nitrite measurement

Renal outer medulla, renal cortex and heart on 0.4% and 4% NaCl diet were extracted. The concentrations of nitrite (NO^{2-}), stable end products of NO, were determined using a Nitrate/Nitrite Colorimetric Assay Kit (Cayman Chemical, USA).

2.8. Urinary analysis

Urinary sodium, potassium, albumin and protein were analyzed as we described previously [33, 34].

2.9. Analysis and visualization of human genomic features

The linkage disequilibrium (LD) regions for blood pressure-associated single nucleotide polymorphisms (SNPs) were defined by HaploReg v4.1 with default settings [35]. Custom Tracks of UCSC genome browser (https://genome.ucsc.edu/cgi-bin/hgCustom; hg38 human genome assembly) were used to visualize several genomic features including defined chromosome regions, chromosome positions of microRNA genes of interest, chromosome potions of LD regions,

SNPs in an LD region, any protein coding genes in the region, and the available H3K4Me1, H3K4Me3 and H3K27Ac histone mark information.

2.10. Statistics

Data were analyzed using Student *t*-test or multiple-group ANOVA. $P < 0.05$ was considered significant unless otherwise indicated. Data are shown as mean $\pm$ SEM.

3. Results

3.1. The abundance of miR-29b and the co-transcribed miR-29a was decreased in multiple tissues in Mir29b-1/a$^{-/-}$ rats

We first examined the abundance of miR-29a and miR-29b in kidney regions, heart and liver in wild-type rats. The abundance of miR-29a in the renal outer medulla was significantly higher than the level in the renal cortex, heart and liver, while the abundance in liver was lower than that in the other tissues (Fig. 1A). For miR-29b, no difference of the abundance was observed among renal outer medulla, renal cortex and heart, while the level of liver was lower (Fig. 1B).

The abundance of miR-29b and the co-transcribed miR-29a were substantially and similarly decreased in the renal outer medulla, renal cortex, heart and liver of *Mir29b-1/a$^{-/-}$* rats (Fig. 1C-F). In *Mir29b-1/a$^{+/-}$* heterozygous mutant rats, the abundance of miR-29b tended to be lower compared to *Mir29b-1/a$^{+/+}$* littermates, but did not reach statistical significance. The abundance of miR-29a from the heterozygous mutant rats was significantly lower in the renal outer medulla than *Mir29b-1/a$^{+/+}$* littermates. The abundance of miR-29c, which is transcribed from a separate gene miR29b-2/c, was unchanged in mutant rats compared to wild-type littermates.
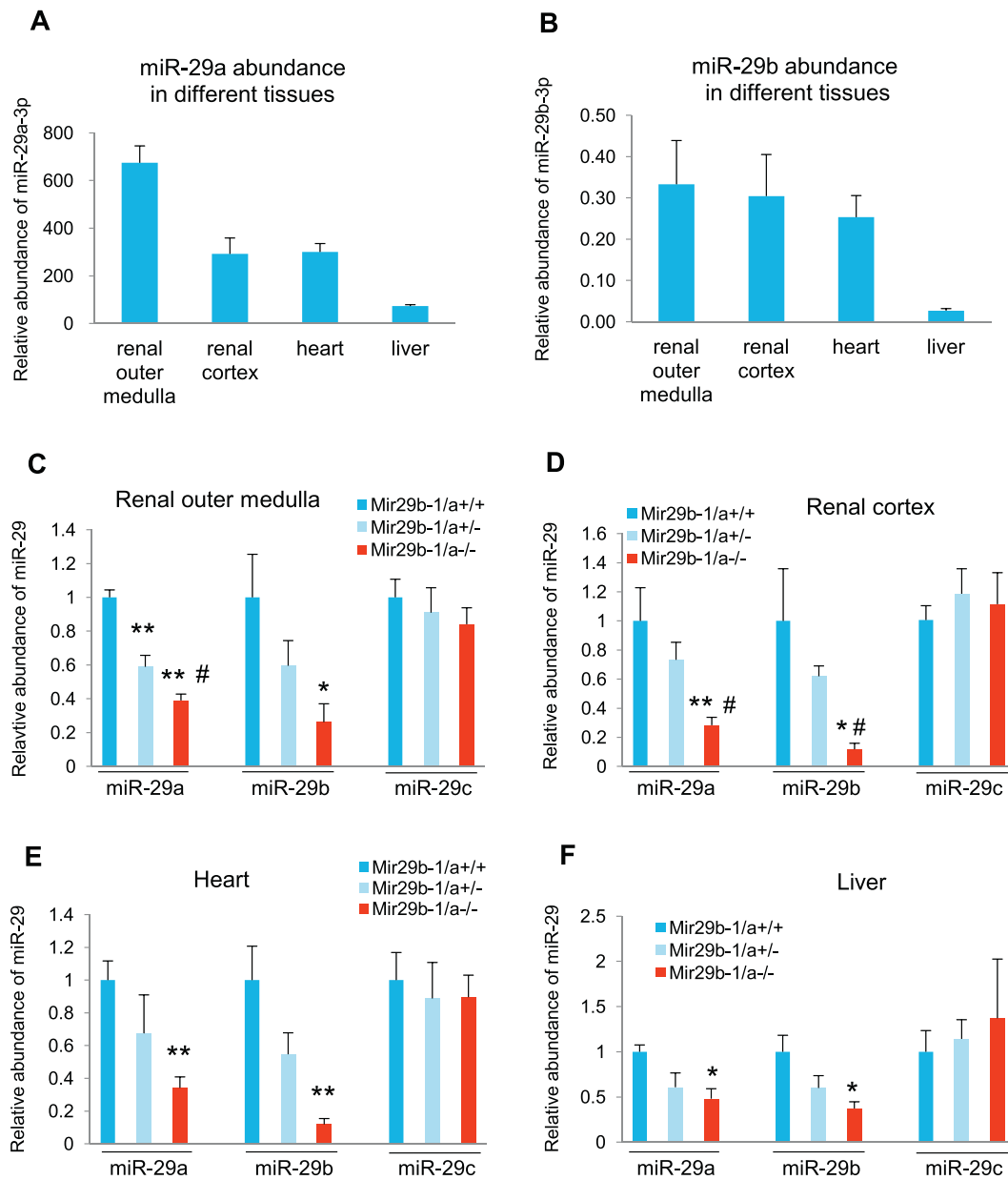
Fig. 1. The abundance of miR-29a and miR-29b is decreased in multiple tissues in *Mir29b-1/a$^{-/-}$* rats. A and B, Abundance of (A) miR-29a and (B) miR-29b in renal outer medulla, renal cortex, heart and liver from *Mir29b-1/a$^{+/+}$* wild-type rats. C to F, Abundance of miR-29a, b and c in (C) renal outer medulla, (D) renal cortex, (E) heart and (F) liver from *Mir29b-1/a$^{+/+}$* wild-type, *Mir29b-1/a$^{+/-}$* heterozygous and *Mir29b-1/a$^{-/-}$* homozygous mutant rats. $n = 6$ for each group, * $P < 0.05$, ** $P < 0.01$ vs *Mir29b-1/a$^{+/+}$*, # $P < 0.05$ vs *Mir29b-1/a$^{+/-}$*, by one-way ANOVA.

These data suggest the miR-29b1 mutation in the $Mir29b\text{-}1/a^{-/-}$ rat leads to a decrease in miR-29a abundance probably because of destabilization of the miR-29b1/a primary transcript, and the residual miR-29b expression likely comes from the miR-29b2 gene. These findings are consistent with our previous findings in arterioles [15] and indicate the $Mir29b\text{-}1/a^{-/-}$ rat is a model of robust miR-29a and miR-29b knockdown in multiple tissues.

3.2. Tissue fibrosis was increased in the renal outer medulla, but not in the renal cortex, heart or liver, of Mir29b-1/a$^{-/-}$ rats on 0.4% NaCl diet

Fibrosis area in kidney regions, heart and liver was assessed by Masson Trichrome staining. The rats were fed with a 0.4% NaCl diet and euthanized when they were eight weeks old, which was prior to the development of overt hypertension. In the renal outer medulla, fibrosis area was significantly increased in $Mir29b\text{-}1/a^{-/-}$ rats compared to $Mir29b\text{-}1/a^{+/+}$ littermates (Fig. 2A and B). No difference was observed between the heterozygous mutant rats and $Mir29b\text{-}1/a^{+/+}$ littermates.

In the renal cortex, heart or liver, fibrosis area tended to be slightly higher in $Mir29b\text{-}1/a^{-/-}$ rats compared to $Mir29b\text{-}1/a^{+/+}$ littermates, but the difference did not reach statistical significance in any of these tissues (Fig. 2C-E). These data suggest that the renal outer medulla might be particularly sensitive to the fibrotic effect of miR-29 insufficiencies.

3.3. Increased level of Lypla1 and reduced nitrite level in the renal outer medulla of Mir29b-1/a$^{-/-}$ rats

In arterioles and endothelial cells, miR-29 increases NO by targeting Lypla1 [15]. The protein level of Lypla1 in the renal outer medulla of $Mir29b\text{-}1/a^{-/-}$ rats on 0.4% NaCl diet was significantly increased compared to $Mir29b\text{-}1/a^{+/+}$ littermates (Fig. 3A). Levels of the stable NO metabolite nitrite in the renal outer medulla of $Mir29b\text{-}1/a^{-/-}$ rats on 0.4% NaCl diet were significantly lower compared to $Mir29b\text{-}1/a^{+/+}$ littermates (Fig. 3B). No difference in either Lypla1 abundance or nitrite level was observed in the renal cortex between $Mir29b\text{-}1/a^{-/-}$ rats
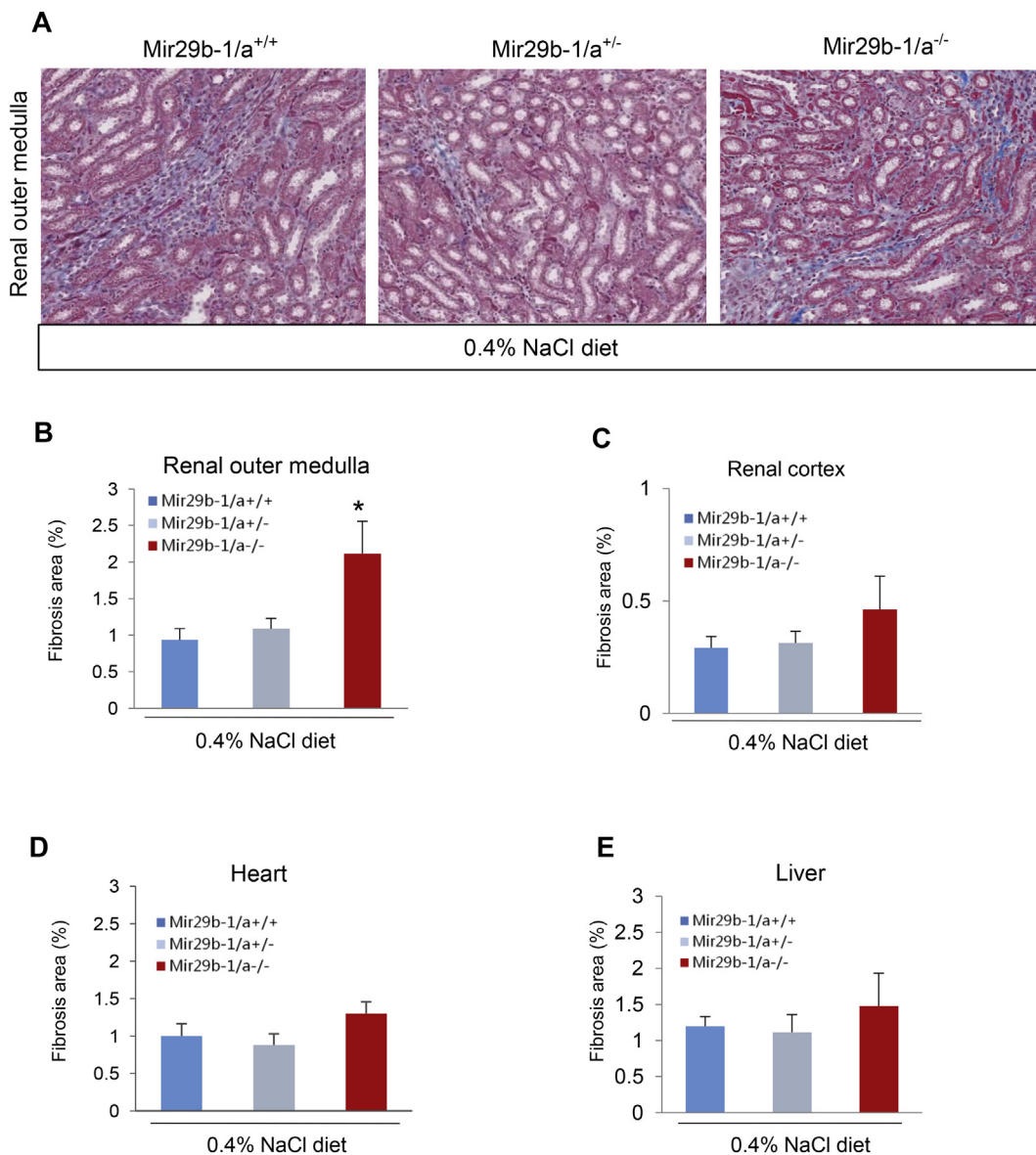
Fig. 2. Fibrosis area specifically in the renal outer medulla is significantly increased in $Mir29b\text{-}1/a^{-/-}$ rats. A, Representative kidney sections illustrating renal outer medulla fibrosis from $Mir29b\text{-}1/a^{+/+}$ wild-type, $Mir29b\text{-}1/a^{+/-}$ heterozygous and $Mir29b\text{-}1/a^{-/-}$ homozygous mutant rats, magnification, ×200. B to E, Quantification of fibrosis area by Masson Trichrome staining in (B) renal outer medulla, (C) renal cortex, (D) heart and (E) liver from $Mir29b\text{-}1/a^{+/+}$ wild-type, $Mir29b\text{-}1/a^{+/-}$ heterozygous and $Mir29b\text{-}1/a^{-/-}$ homozygous mutant rats on 0.4% NaCl diet. $n = 7$ or 8 for each group, * P < 0.05 vs $Mir29b\text{-}1/a^{+/+}$, by one-way ANOVA.
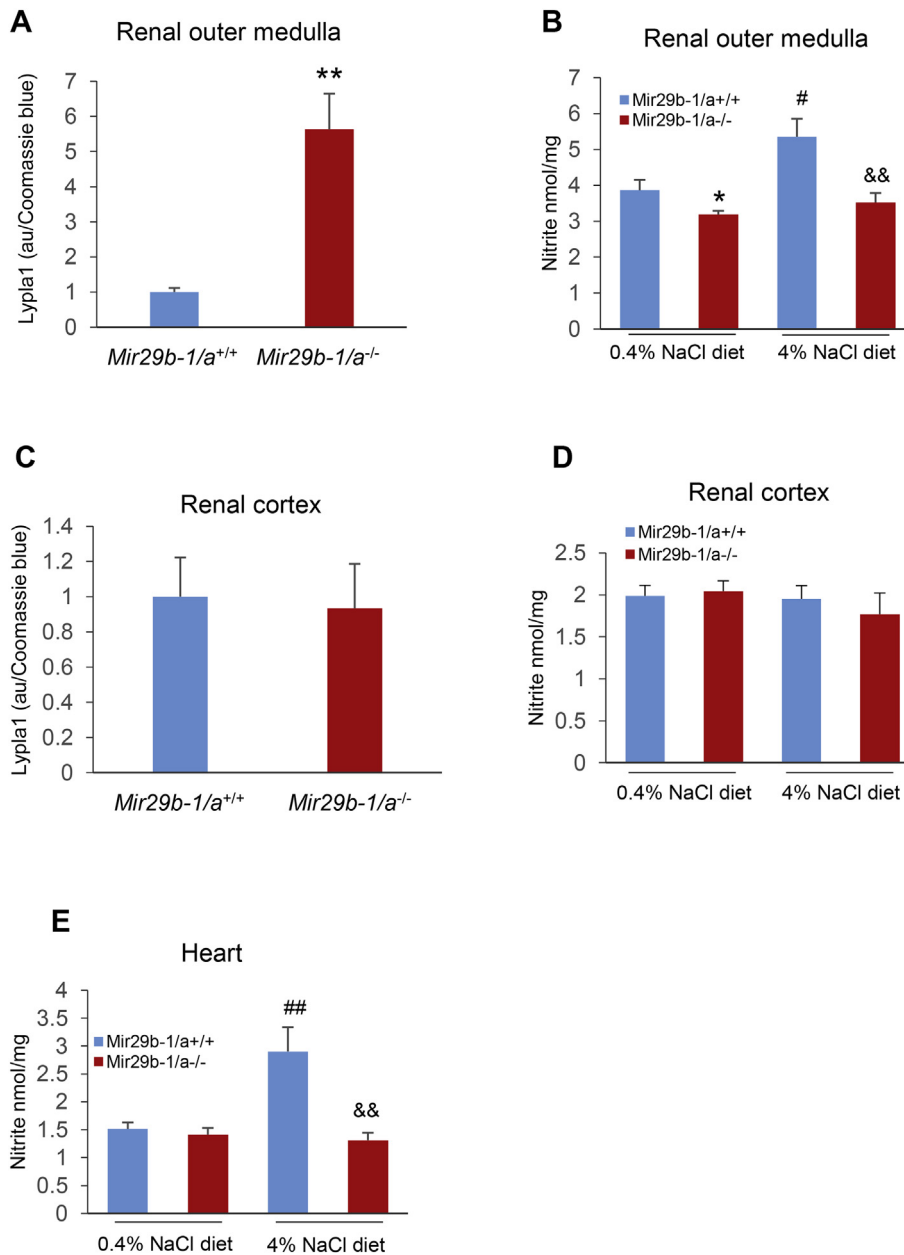
Fig. 3. Lypla1 protein level is up-regulated and NO level reduced in the renal outer medulla of *Mir29b-1/a$^{−/−}$*rats. A and B, Quantification of (A) Lypla1 protein level on 0.4% NaCl diet and (B) level of nitrite, a stable NO metabolites, on 0.4% and 4% NaCl diet in renal outer medulla from *Mir29b-1/a$^{+/+}$* and *Mir29b-1/a$^{−/−}$* rats. C and D, (C) Quantification of Lypla1 protein level on 0.4% NaCl and (D) level of nitrite on 0.4% and 4% NaCl diet in renal cortex. E, Level of nitrite in the heart. $n = 5$ or 6 for each group, $^{*}P < 0.05$, $^{**} P < 0.01$ vs *Mir29b-1/a$^{+/+}$* on 0.4% NaCl diet, by *t*-test. $^{\#}P < 0.05$, $^{\#\#}P < 0.01$ vs *Mir29b-1/a$^{+/+}$* on 0.4% NaCl diet, $^{\&\&}P < 0.01$ vs *Mir29b-1/a$^{+/+}$* on 4% NaCl diet by one way ANOVA.

and *Mir29b-1/a$^{+/+}$* littermates on 0.4% NaCl diet (Fig. 3C and D). After 14 days of a 4% NaCl diet, nitrite levels in the renal outer medulla of *Mir29b-1/a$^{+/+}$* were increased compared with the level on the 0.4% NaCl diet, while in *Mir29b-1/a$^{−/−}$* rats, nitrite levels remained lower compared with *Mir29b-1/a$^{+/+}$* littermates. Furthermore, nitrite levels in the heart of *Mir29b-1/a$^{+/+}$* rats were significantly increased after the diet switch. Nitrite levels in *Mir29b-1/a$^{−/−}$* rats on the 4% NaCl diet were significantly lower than those in *Mir29b-1/a$^{+/+}$* littermates (Fig. 3E).

3.4. Fibrosis remained higher in the renal outer medulla and became higher in the heart in Mir29b-1/a$^{−/−}$ rats on 4% NaCl diet

The *Mir29b-1/a$^{−/−}$* rat was developed on the genetic background of the SS-Chr13^{BN} rat. SS-Chr13^{BN} rats are consomic rats derived from the

SS rats and exhibit attenuated salt-induced hypertension and renal injury compared to SS rats. *Mir29b-1/a$^{−/−}$* rats on a 4% NaCl diet exhibited exacerbated hypertension compared to *Mir29b-1/a$^{+/+}$* littermates, which were essentially SS-Chr13^{BN}rats [15]. We assessed tissue fibrosis in *Mir29b-1/a$^{−/−}$* rats two weeks after switching the rat diet from one containing 0.4% NaCl to 4% NaCl. Masson Trichrome staining showed fibrosis area in *Mir29b-1/a$^{−/−}$* rats was significantly higher in the renal outer medulla compared to *Mir29b-1/a$^{+/+}$* littermates or heterozygous mutant rats after two weeks of the 4% NaCl diet (Fig. 4A and B). In the renal cortex, no difference was observed between *Mir29b-1/a$^{−/−}$* rats and *Mir29b-1/a$^{+/+}$* littermates (Fig. 4C). While no changes of fibrosis were observed in the heart of *Mir29b-1/a$^{−/−}$* rats on the 0.4% NaCl diet, fibrosis area in the heart of *Mir29b-1/a$^{−/−}$* rats was greatly increased compared to *Mir29b-1/a$^{+/+}$* littermates after two weeks on the 4% NaCl diet (Fig. 4D and E).
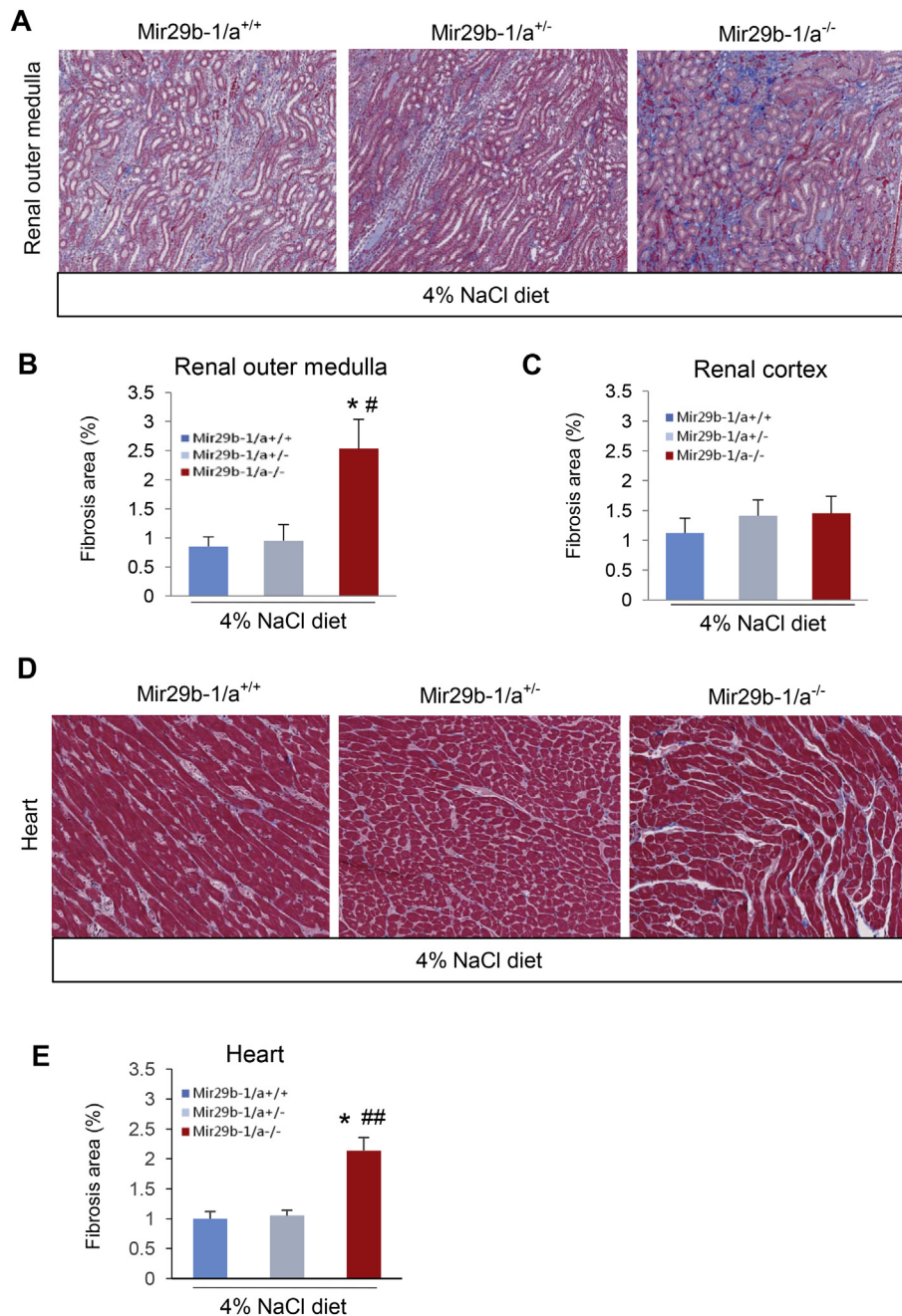
Fig. 4. Fibrosis area in the renal outer medulla and heart is increased in *Mir29b-1/a$^{-/-}$* rats fed a 4% NaCl diet. A, Representative kidney sections illustrating renal outer medulla fibrosis from *Mir29b-1/a$^{+/+}$* wild-type, *Mir29b-1/a$^{+/-}$* heterozygous and *Mir29b-1/a$^{-/-}$* homozygous mutant rats, magnification, ×200. B and C, Quantification of fibrosis area by Masson Trichrome staining in (B) renal outer medulla and (C) renal cortex from *Mir29b-1/a$^{+/+}$*, *Mir29b-1/a$^{+/-}$* and *Mir29b-1/a$^{-/-}$* rats fed a 4% NaCl diet for two weeks. D and E, (D) Representative heart sections and (E) Quantification by Masson Trichrome staining illustrating heart fibrosis from *Mir29b-1/a$^{+/+}$*, *Mir29b-1/a$^{+/-}$* and *Mir29b-1/a$^{-/-}$* rats fed a 4% NaCl diet for two weeks. n = 7 or 8 for each group, * P < 0.05 vs *Mir29b-1/a$^{+/+}$*, # P < 0.05, ## P < 0.01 vs *Mir29b-1/a$^{+/-}$*, by one-way ANOVA.

3.5. 24 h urine volume and urinary sodium excretion are decreased by the Mir29b1 mutation

Urine samples were collected in metabolic cages from rats either on 0.4% NaCl or after two weeks of 4% NaCl diet. 24 h urine volume on 0.4% NaCl diet was 6.8 ± 0.2 ml, 5.3 ± 0.2 ml and 3.0 ± 0.8 ml for *Mir29b-1/a$^{+/+}$*, *Mir29b-1/a$^{+/-}$* and *Mir29b-1/a$^{-/-}$* rat respectively (Fig. 5A). Although the difference between genotypes did not reach statistical significance, the result showed a trend of reduced urine volume in rats with *Mir29b1* mutation. After two weeks of 4% NaCl diet, 24 h urine volume in *Mir29b-1/a$^{+/-}$* and *Mir29b-1/a$^{-/-}$* rats was significantly lower

compared with *Mir29b-1/a$^{+/+}$* littermates. Rat body weight increased during the experimental period. No difference was observed between genotypes on 0.4% NaCl diet, but body weight of *Mir29b-1/a$^{-/-}$* rats were significantly lower compared with *Mir29b-1/a$^{+/+}$* or *Mir29b-1/a$^{+/-}$* rats (Fig. 5B). After being normalized by body weight, urine volume remains significantly lower in *Mir29b-1/a$^{-/-}$* and *Mir29b-1/a$^{+/-}$* rats compared with *Mir29b-1/a$^{+/+}$* rats. Urinary sodium excretion was not significantly different between genotypes on 0.4% NaCl diet. However, on 4% NaCl diet, it was significantly lower in *Mir29b-1/a$^{-/-}$* and *Mir29b-1/a$^{+/-}$* rats compared with wild-type littermates (Fig. 5C). On the 0.4% NaCl diet, urinary excretion of potassium was lower in
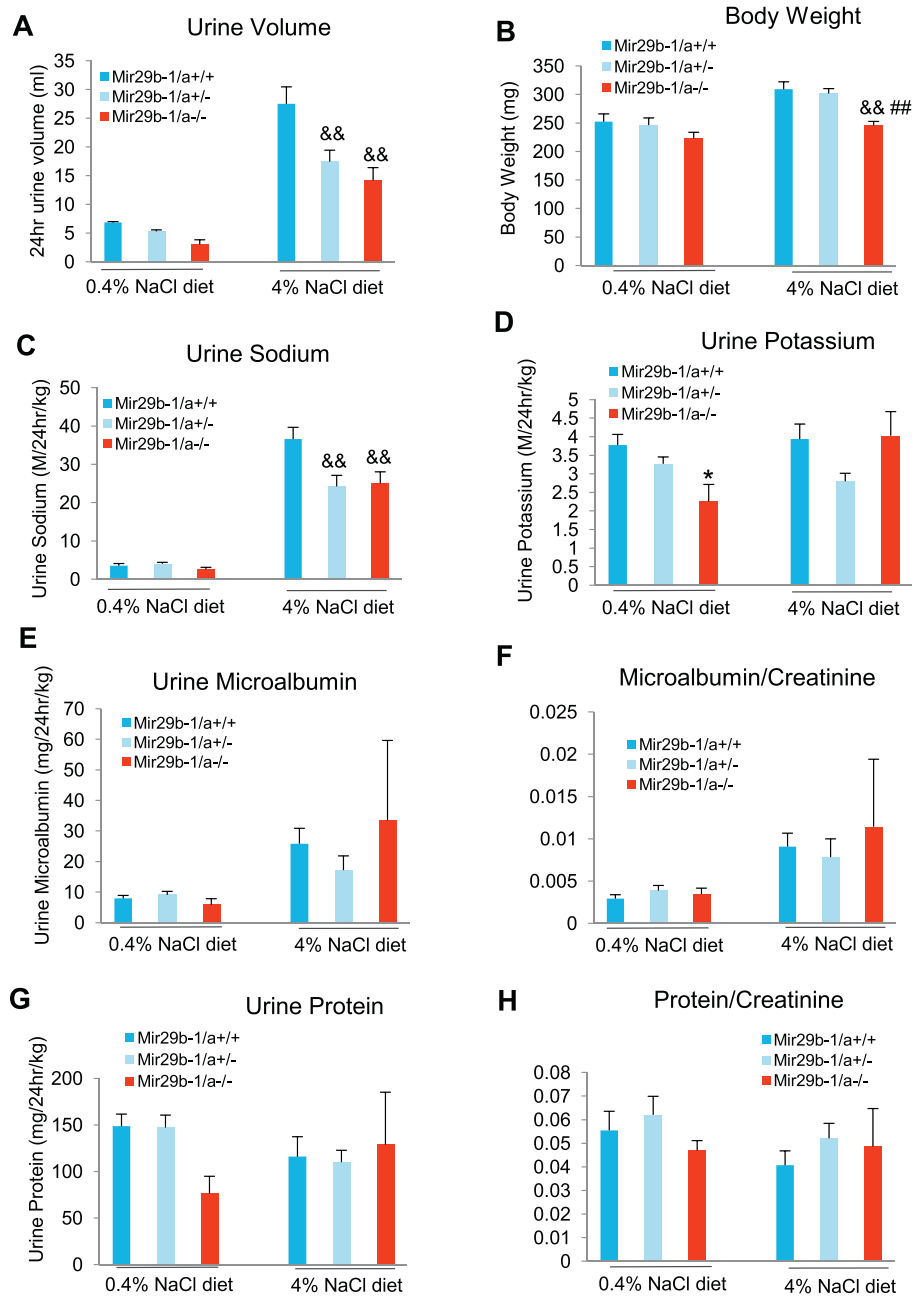
Fig. 5. Urinary analysis of *Mir29b-1/a$^{-/-}$* rats on 0.4% NaCl or 4% NaCl diet. 24 h urine was collected in metabolic cages from individual rats on 0.4% NaCl diet. After a switch to a 4% NaCl diet for two weeks, 24 h urine was collected again. Urine volume and body weight were recorded, and urine microalbumin, protein, creatinine, sodium and potassium were measured. A, 24 h urine volume. B, Body weight of rats. C, Urine Sodium. D, Urine potassium. E, Urine microalbumin. F, Microalbumin/Creatinine ratios. G, Urine protein. H, Protein/Creatinine ratios. n = 6 for *Mir29b-1/a$^{+/+}$* or *Mir29b-1/a$^{-/-}$* rats, and *n* = 9 for *Mir29b-1/a$^{+/-}$* rats. * $P < 0.05$ vs *Mir29b-1/a$^{+/+}$* on 0.4% NaCl diet, $^{\&\&}$ $P < 0.01$ vs *Mir29b-1/a$^{+/+}$* on 4% NaCl diet, $^{\#\#}$ $P < 0.01$ vs *Mir29b-1/a$^{+/-}$* on 4% NaCl diet, by two-way repeated measures ANOVA.

Mir29b-1/a$^{-/-}$ rats. After diet switch, urinary excretion of potassium was unchanged in *Mir29b-1/a$^{+/+}$* and *Mir29b-1/a$^{+/-}$* rats, but it was significantly increased in *Mir29b-1/a$^{-/-}$* rats (comparing the red bar on 4% to the red bar on 0.4% in Fig. 5D). No statistic difference was observed between genotypes on 4% NaCl diet (Fig. 5D).

The presence of albuminuria or proteinuria is a sign of kidney damage [36]. Microalbuminuria was significantly exacerbated in rats after two weeks of the 4% NaCl diet. However, no significant difference was observed between *Mir29b-1/a$^{+/+}$* and mutant rats (Fig. 5E, F). Total urinary protein was not significantly different between diets or genotypes (Fig. 5G, H).

3.6. Human miR-29 genes are located in proximity with blood pressure-associated SNPs

An analysis of 283 human blood pressure-associated SNPs identified by genome-wide association studies and 1870 known human microRNA precursors identified 16 microRNAs located within the LD regions of blood pressure-associated SNPs [35]. The mir-29b-2 gene and miR-29c gene, which form a gene cluster, were located within the 97,745 bp LD region of the blood pressure-associated SNP rs12731740 (Fig. 6). The LD region contained several peaks of enhancer marks H3K4Me1 and H3K27Ac (Fig. 6). miR-29b1/a gene did not overlap
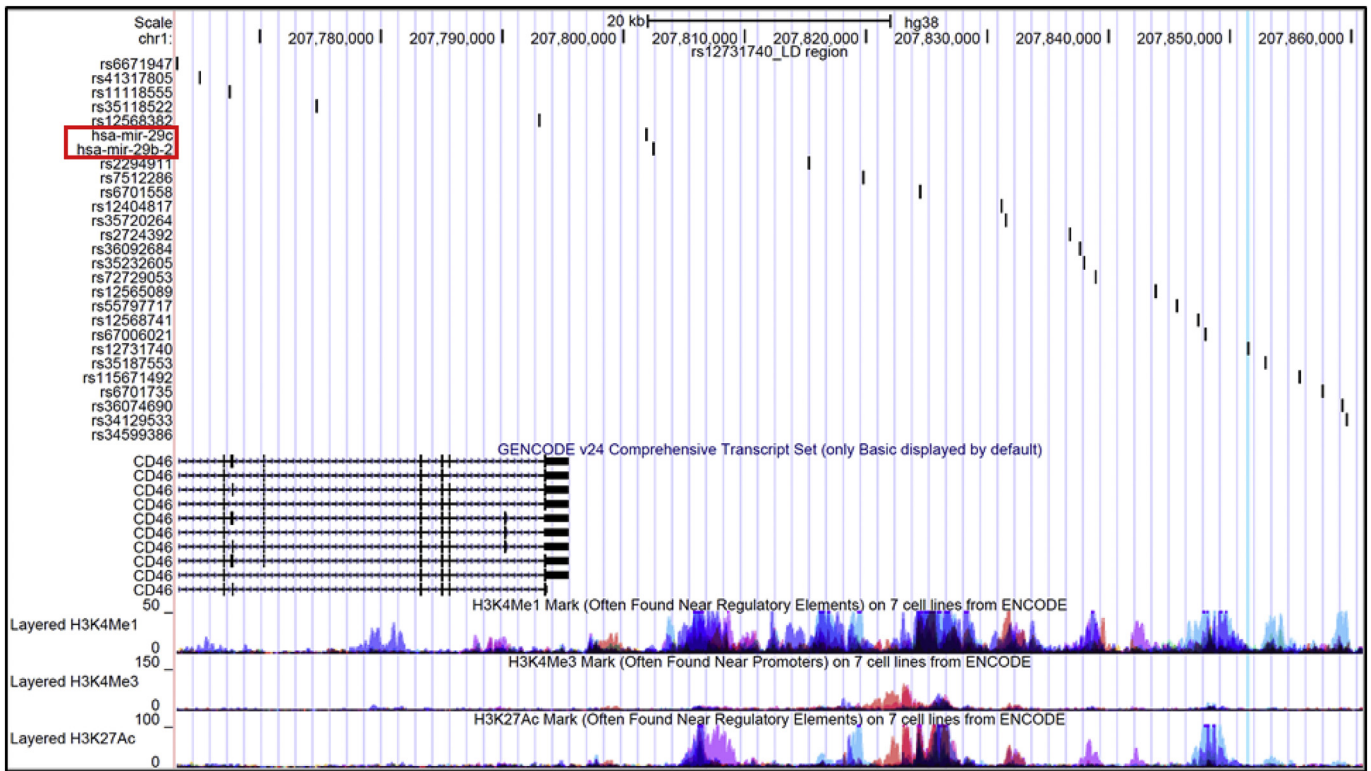
Fig. 6. Human miR-29b2/c gene overlaps with the linkage disequilibrium (LD) region of a blood pressure-associated SNP, rs12731740. Custom tracks built from the UCSC genome browser are shown. The chromosome region of the LD block is shown, together with the locations of miR-29b-2 and miR-29c, all SNPs in LD with rs12731740, and known peaks of histone marks H3K4Me1 (enhancer), H3K4Me3 (promoter) and H3K27Ac (enhancer).

with a blood pressure-associated LD region but is located approximately 454 kb and 853 kb from the LD regions of blood pressure-associated SNPs rs13238550 and rs11556924, respectively.

4. Discussion

Although miR-29 has been proven to target several extracellular matrix genes [1], the effect of miR-29 on tissue fibrosis has been somewhat controversial. Several groups have used genetic depletion of miR-29 to evaluate its role in tissue fibrosis and other physiological processes and diseases. No overt lesions were noted in the liver of liver-specific miR29ab1 knockout mice under normal conditions [37]. After liver injury was induced by carbon tetrachloride, increased hepatic fibrosis and carcinogenesis was observed in the miR29ab1 knockout mice compared with their wild-type controls. In a study by Sassi, et al., mouse lines with partial deficiency of miR-29 variants, miR-29 ab1 $^{-/-}$ b2c $^{+/-}$ or ab1 $^{+/+}$ b2c $^{-/-}$ genotype was generated due to high mortality induced by complete genetic loss of both miR-29 clusters (miR-29, a/b1, and b2/c) [38]. The knockout mice did not show any cardiac phenotype under basal conditions. In a left ventricular pressure overload model induced by transverse aortic constriction, miR-29 was shown to promote hypertrophic growth of cardiac myocytes in vivo, together with an increase, rather than a reduction, of cardiac fibrosis [38]. In addition, the authors did not observe an increase of Sirius Red staining for extracellular matrix in miR-29 ab1 $^{-/-}$ b2c $^{+/-}$ mice in liver, kidney or lung [38].

In the present study, *Mir29b1* homozygous mutation in rats induced significantly increased fibrosis only in the renal outer medulla for rats on a 0.4% NaCl diet, not in the renal cortex, liver, or heart. An increased fibrosis was observed in the heart of *Mir29b-1/a*$^{-/-}$ rats after two weeks of a 4% NaCl diet, which might be the result of the exacerbated hypertension in *Mir29b-1/a*$^{-/-}$ rats [15] or the hypertension in combination with the loss of miR-29. Fibrosis in the renal cortex and liver remain

similar across genotypes on the high-salt diet. Consistent with a particularly important role for miR-29 in the regulation of fibrosis in the renal medulla, miR-29 was elevated only in renal medulla in SS-Chr13^{BN} rats, but not in renal cortex, after a switch to a high salt diet [11].

Together, these studies suggest the effect of miR-29 on fibrosis might be dependent on tissue type and disease context.

miR-29 increases NO in arterioles and endothelial cells by targeting Lypla1 [15]. In the present study, Lypla1 was up-regulated and nitrite decreased in the renal outer medulla of *Mir29b-1/a*$^{-/-}$ rats, but not in the renal cortex. It suggests the miR-29/Lypla1/NO pathway might be involved in the functional role of miR-29 in the renal outer medulla. In the heart, no difference of nitrite level was observed between genotypes on the 0.4% NaCl diet, but on the 4% NaCl diet, nitrite level was lower in *Mir29b-1/a*$^{-/-}$ rats. It suggests the miR-29/NO pathway might also be involved in the development of fibrosis in the heart after the diet switch. Tissue NO has been shown to have protective effect on tissue injury and fibrosis in previous studies. For example, in the liver, NO plays a prominent role in the protective effect in bile duct ligation-induced liver fibrosis in rats [22]. In addition, a marked decrease in eNOS phosphorylation and NO level was involved in development of isoproterenol induced myocardial fibrosis [23].

In kidney, NO participates in several vital processes, including the regulation of glomerular and medullary hemodynamics, the tubuloglomerular feedback response, renin release, and the extracellular fluid volume [24]. In addition, thick ascending limb (TAL) and the connecting tubules (CDs) are rich sources of NO and the primary site of NO-mediated inhibition of tubular reabsorption during increased renal perfusion pressure [39]. Blockade of NO attenuated the increases in renal medullary blood flow and Na$^+$ excretion during increased renal perfusion pressure. Renal medullary blood flow is a major determinant of Na$^+$ excretion and blood pressure [40, 41]. Proximal tubule is the primary site in the kidney that synthesizes arginine from

citrulline, suggesting that the substrate of NO synthesis is abundant [25]. However, the effects of NO in the proximal tubule are more controversial, with reports of inhibiting or stimulating Na$^+$ reabsorption [25, 39]. It appears that the reduced NO level in the renal outer medulla induced by *Mir29b1* mutation might play a role in the lower urine volume and urinary sodium excretion observed in the present study. Other mechanisms might also be involved. For example, in the intestines, miR-29 was shown to increase intestinal permeability by targeting nuclear factor-κB-repressing factor and Claudin 1 [42]. Paracellular permeability plays significant role in the regulation of renal tubular reabsorption of sodium and fluid [43, 44],.

The overlap of miR-29b2/c with the LD region of a blood pressure-associated SNP suggests miR-29b2/c might be regulated by common genetic variants associated with blood pressure. The presence of histone marks of enhancers in the LD region further supports this possibility. Although less certain, miR-29b1/a could also be regulated by blood pressure-associated genetic variants since it is located <1 Mb from LD regions of two blood pressure-associated SNPs [35]. Even if miR-29b2/c is regulated by blood pressure-associated SNPs and miR-29b1/a is not, it would still support the human relevance of the findings we made using *Mir29b-1/a$^{-/-}$* rats. That is because the effect of miR-29 on NO and tissue fibrosis is a common effect of all miR-29 isomers.

Exciting progress is being made in the development of miR-29-based therapeutic approaches [45]. The present study highlights the importance of considering the tissue- and disease context-specificity of the effect of miR-29 as well as miR-29 effects that are not yet well-understood, such as effects on fluid and electrolyte balance.

Word count for the body of the paper: 3190 words.

Sources of funding

Author contributions

HX, GZ and ML designed experiments. HX and GZ performed experiments. AMG maintained and genotyped mutant rats. KU, DMJ and YL assisted experiments. YL performed the bioinformatic analysis. MEW provided input for design and analysis. HX and ML wrote the manuscript.

Disclosures

None.

References

[1] Kriegel, A.J., Liu, Y., Fang, Y., Ding, X., Liang, M., 2012]. The miR-29 family: genomics, cell biology, and relevance to renal and cardiovascular injury. Physiol Genomics 44 (4), 237–244.

[2] O'Reilly, S., 2016]. MicroRNAs in fibrosis: opportunities and challenges. Arthritis Res Ther 18, 11.

[3] van Rooij, E., Sutherland, L.B., Thatcher, J.E., et al., 2008]. Dysregulation of microRNAs after myocardial infarction reveals a role of miR-29 in cardiac fibrosis. Proc Natl Acad Sci U S A 105 (13027–32. 3).

[4] Abonnenc, M., Nabeebaccus, A.A., Mayr, U., et al., 2013]. Extracellular matrix secretion by cardiac fibroblasts: role of microRNA-29b and microRNA-30c. Circ Res 113 (10), 1138–1147.

[5] Roderburg, C., Urban, G.W., Bettermann, K., et al., 2011]. Micro-RNA profiling reveals a role for miR-29 in human and murine liver fibrosis. Hepatology 53 (1), 209–218.

[6] Matsumoto, Y., Itami, S., Kuroda, M., Yoshizato, K., Kawada, N., Murakami, Y., 2016]. MiR-29a assists in preventing the activation of human stellate cells and promotes recovery from liver fibrosis in mice. Mol. Ther. 24 (10), 1848–1859.

[7] Wang, B., Komers, R., Carew, R., et al., 2012]. Suppression of microRNA-29 expression by TGF-β1 promotes collagen expression and renal fibrosis. J Am Soc Nephrol 23, 252–265.

[8] Fang, Y., Yu, X., Liu, Y., et al., 2013]. miR-29c is downregulated in renal interstitial fibrosis in humans and rats and restored by HIF-α activation. Am J Physiol Renal Physiol 304 (10), F1274–F1282.

[9] Zhu, J.N., Chen, R., Fu, Y.H., et al., 2013]. Smad3 inactivation and MiR-29b upregulation mediate the effect of carvedilol on attenuating the acute myocardium infarction-induced myocardial fibrosis in rat. PLoS One 8, e75557.

[10] Knabel, M.K., Ramachandran, K., Karhadkar, S., et al., 2015]. Systemic delivery of scAAV8-encoded MiR-29a ameliorates hepatic fibrosis in carbon tetrachloride-treated mice. PLoS One 10, e0124411.

[11] Liu, Y., Taylor, N.E., Lu, L., et al., 2010]. Renal medullary microRNAs in Dahl salt-sensitive rats: miR-29b regulates several collagens and related genes. Hypertension 55 (4), 974–982.

[12] Kotchen, T.A., Cowley Jr., A.W., Frohlich, E.D., 2013 Mar 28]. Salt in health and disease–a delicate balance. N Engl J Med 368 (13), 1229–1237.

[13] Cowley Jr., A.W., Liang, M., Roman, R.J., Greene, A.S., Jacob, H.J., 2004]. Consomic rat model systems for physiological genomics. Acta Physiol Scand 181 (4), 585–592.

[14] Cowley Jr., A.W., Roman, R.J., Kaldunski, M.L., et al., 2001]. Brown Norway chromosome 13 confers protection from high salt to consomic Dahl S rat. Hypertension 37, 456–461.

[15] Widlansky, M.E., Jensen, D.M., Wang, J., et al., 2018]. miR-29 contributes to normal endothelial function and can restore it in cardiometabolic disorders. EMBO Mol Med https://doi.org/10.15252/emmm.201708046 pii: e8046.

[16] Cowley Jr., A.W., 1992]. Long-term control of arterial blood pressure. Physiol Rev 72 (1), 231–300.

[17] Cowley Jr I, A.W., Mattson, D.L., Lu, S., Roman, R.J., 1995]. The renal medulla and hypertension. Hypertension 25 (4 Pt 2), 663–673.

[18] Cowley Jr I, A.W., Roman, R.J., 1996]. The role of the kidney in hypertension. JAMA 275 (20), 1581–1589.

[19] Guyton, A.C., 1991]. Blood pressure control—special role of the kidneys and body fluids. Science 252 (5014), 1813–1816.

[20] Garrett, M.R., Dene, H., Rapp, J.P., 2003]. Time-course genetic analysis of albuminuria in Dahl salt-sensitive rats on low-salt diet. J Am Soc Nephrol 14 (5), 1175–1187.

[21] Johnson, R.J., Gordon, K.L., Giachelli, C., Kurth, T., Skelton, M.M., Cowley Jr., A.W., 2000]. Tubulo interstitial injury and loss of nitric oxide synthases parallel the development of hypertension in the Dahl-SS rat. J Hypertens 18 (10), 1497–1505.

[22] Mohamed, Y.S., Ahmed, L.A., Salem, H.A., Agha, A.M., 2018]. Role of nitric oxide and KATP channel in the protective effect mediated by nicorandil in bile duct ligation-induced liver fibrosis in rats. Biochem Pharmacol 151, 135–142.

[23] Wang, Q., Zhang, Y., Li, D., et al., 2016]. Transgenic overexpression of transient receptor potential vanilloid subtype 1 attenuates isoproterenol-induced myocardial fibrosis in mice. Int J Mol Med 38 (2), 601–609.

[24] Kone, B.C., 1997]. Nitric oxide in renal health and disease. Am J Kidney Dis 30 (3), 311–333.

[25] Liang, M., Knox, F.G., 2000]. Production and functional roles of nitric oxide in the proximal tubule. Am J Physiol Regul Integr Comp Physiol 278 (5), R1117–R1124.

[26] Garvin, J.L., Herrera, M., Ortiz, P.A., 2011]. Regulation of renal NaCl transport by nitric oxide, endothelin, and ATP: clinical implications. Annu Rev Physiol 73:359–376. https://doi.org/10.1146/annurev-physiol-012110-142247.

[27] Pollock, J.S., Pollock, D.M., 2008]. Endothelin and NOS1/nitric oxide signaling and regulation of sodium homeostasis. Curr Opin Nephrol Hypertens 17 (1), 70–75.

[28] Geurts, A.M., Cost, G.J., Rémy, S., et al., 2010]. Generation of gene-specific mutated rats using zinc-finger nucleases. Methods Mol Biol 597, 211–225.

[29] Kriegel, A.J., Liu, Y., Cohen, B., Usa, K., Liu, Y., Liang, M., 2012]. MiR-382 targeting of kallikrein 5 contributes to renal inner medullary interstitial fibrosis. Physiol Genomics 44 (4), 259–267.

[30] Tian, Z., Greene, A.S., Pietrusz, J.L., Matus, I.R., Liang, M., 2008]. microRNA-target pairs in rat kidneys identified through microRNA microarray, proteomic, and bioinformatic analysis. Genome Res 18, 404–411.

[31] Liu, Y., Singh, R.J., Usa, K., Netzel, B.C., Liang, M., 2008]. Renal medullary 11beta-hydroxysteroid dehydrogenase type 1 in Dahl salt-sensitive hypertension. Physiol Genomics 36, 52–58.

[32] Usa, K., Liu, Y., Geurts, A.M., et al., 2017]. Elevation of fumarase attenuates hypertension and can result from a nonsynonymous sequence variation or increased expression depending on rat strain. Physiol Genomics 49 (9), 496–504.

[33] Mladinov, D., Liu, Y., Mattson, D.L., Liang, M., 2013]. MicroRNAs contribute to the maintenance of cell-type-specific physiological characteristics: miR-192 targets Na+/K+-ATPase β1. Nucleic Acids Res 41 (2), 1273–1283.

[34] Liang, M., Lee, N.H., Wang, H., et al., 2008]. Molecular networks in Dahl salt-sensitive hypertension based on transcriptome analysis of a panel of consomic rats. Physiol Genomics 34 (1), 54–64.

[35] Liu, Y., Usa, K., Wang, F., et al., 2018]. MicroRNA-214-3p in the kidney contributes to the development of hypertension. J Am Soc Nephrol https://doi.org/10.1681/ASN.2018020117 Jul 26. pii: ASN.2018020117. [Epub ahead of print].

[36] Gorriz, J.L., Martinez-Castelao, A., 2012]. Proteinuria: detection and role in native renal disease progression. Transplant Rev (Orlando) 26 (1), 3–13.

[37] Kogure, T., Costinean, S., Yan, I., Braconi, C., Croce, C., Patel, T., 2012]. Hepatic miR-29ab1 expression modulates chronic hepatic injury. J Cell Mol Med 16 (11), 2647–2654.

[38] Sassi, Y., Avramopoulos, P., Ramanujam, D., et al., 2017]. Cardiac myocyte miR-29 promotes pathological remodeling of the heart by activating Wnt signaling. Nat Commun 8 (1), 1614.

[39] Carlström, M., Wilcox, C.S., Arendshorst, W.J., 2015]. Renal autoregulation in health and disease. Physiol Rev 95 (2), 405–511.

[40] Cowley Jr., A.W., 2008]. Renal medullary oxidative stress, pressure-natriuresis, and hypertension. Hypertension 52 (5), 777–786.

[41] Cowley Jr., A.W., Mattson, D.L., Lu, S., Roman, R.J., 1995]. The renal medulla and hypertension. Hypertension 25 (4 Pt 2), 663–673.

[42] Zhou Q, Costinean S, Croce CM, et al. MicroRNA 29 targets nuclear factor-κB-repressing factor and Claudin 1 to increase intestinal permeability. Gastroenterology. 2015;148(1):158–169.e8.

[43] Liang, M., Ramsey, C.R., Knox, F.G., 1999]. The paracellular permeability of opossum kidney cells, a proximal tubule cell line. Kidney Int 56 (6), 2304–2308.

[44] Ramsey, C.R., Berndt, T.J., Knox, F.G., 1998]. Effect of volume expansion on the paracellular flux of lanthanum in the proximal tubule. J Am Soc Nephrol 9 (7), 1147–1152.

[45] Montgomery, R.L., Yu, G., Latimer, P.A., et al., 2014]. MicroRNA mimicry blocks pulmonary fibrosis. EMBO Mol Med 6 (10), 1347–1356.